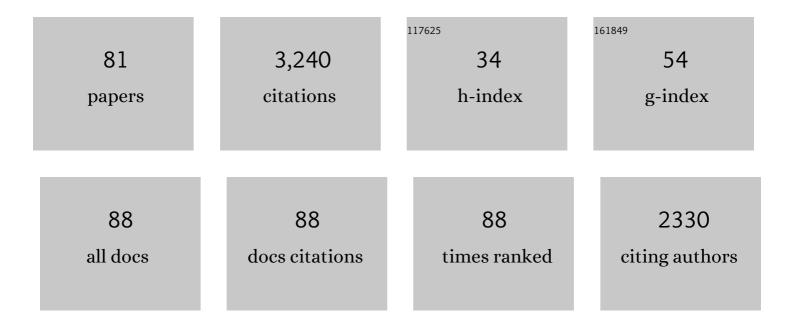
Loren B Andreas

List of Publications by Year in descending order

Source: https://exaly.com/author-pdf/8720733/publications.pdf Version: 2024-02-01



#	Article	IF	CITATIONS
1	Rapid Proton-Detected NMR Assignment for Proteins with Fast Magic Angle Spinning. Journal of the American Chemical Society, 2014, 136, 12489-12497.	13.7	254
2	Structure of fully protonated proteins by proton-detected magic-angle spinning NMR. Proceedings of the United States of America, 2016, 113, 9187-9192.	7.1	224
3	Magic Angle Spinning NMR of Proteins: High-Frequency Dynamic Nuclear Polarization and ¹ H Detection. Annual Review of Biochemistry, 2015, 84, 465-497.	11.1	128
4	High-resolution proton-detected NMR of proteins at very fast MAS. Journal of Magnetic Resonance, 2015, 253, 36-49.	2.1	122
5	NMR Spectroscopic Assignment of Backbone and Sideâ€Chain Protons in Fully Protonated Proteins: Microcrystals, Sedimented Assemblies, and Amyloid Fibrils. Angewandte Chemie - International Edition, 2016, 55, 15504-15509.	13.8	116
6	Paramagnet induced signal quenching in MAS–DNP experiments in frozen homogeneous solutions. Journal of Magnetic Resonance, 2014, 240, 113-123.	2.1	106
7	Structure and Mechanism of the Influenza A M2 _{18–60} Dimer of Dimers. Journal of the American Chemical Society, 2015, 137, 14877-14886.	13.7	103
8	Structure of outer membrane protein G in lipid bilayers. Nature Communications, 2017, 8, 2073.	12.8	91
9	Expanding the horizons for structural analysis of fully protonated protein assemblies by NMR spectroscopy at MAS frequencies above 100ÂkHz. Solid State Nuclear Magnetic Resonance, 2017, 87, 117-125.	2.3	88
10	Resolution and polarization distribution in cryogenic DNP/MAS experiments. Physical Chemistry Chemical Physics, 2010, 12, 5861.	2.8	87
11	Magic Angle Spinning NMR Investigation of Influenza A M2 _{18â^'60} : Support for an Allosteric Mechanism of Inhibition. Journal of the American Chemical Society, 2010, 132, 10958-10960.	13.7	82
12	Dynamic Nuclear Polarization Study of Inhibitor Binding to the M2 _{18–60} Proton Transporter from Influenza A. Biochemistry, 2013, 52, 2774-2782.	2.5	66
13	1H magic-angle spinning NMR evolves as a powerful new tool for membrane proteins. Journal of Magnetic Resonance, 2018, 287, 140-152.	2.1	65
14	Combining DNP NMR with segmental and specific labeling to study a yeast prion protein strain that is not parallel in-register. Proceedings of the National Academy of Sciences of the United States of America, 2017, 114, 3642-3647.	7.1	63
15	Solid-State NMR Structure Determination from Diagonal-Compensated, Sparsely Nonuniform-Sampled 4D Proton–Proton Restraints. Journal of the American Chemical Society, 2014, 136, 11002-11010.	13.7	61
16	2H-DNP-enhanced 2H–13C solid-state NMR correlation spectroscopy. Physical Chemistry Chemical Physics, 2010, 12, 5872.	2.8	55
17	Magic-Angle-Spinning NMR of the Drug Resistant S31N M2 Proton Transporter from Influenza A. Journal of the American Chemical Society, 2012, 134, 7215-7218.	13.7	55
18	Selective ¹ H– ¹ H Distance Restraints in Fully Protonated Proteins by Very Fast Magic-Angle Spinning Solid-State NMR. Journal of Physical Chemistry Letters, 2017, 8, 2399-2405.	4.6	54

#	Article	IF	CITATIONS
19	Conformational dynamics in crystals reveal the molecular bases for D76N beta-2 microglobulin aggregation propensity. Nature Communications, 2018, 9, 1658.	12.8	53
20	A β-barrel for oil transport through lipid membranes: Dynamic NMR structures of AlkL. Proceedings of the United States of America, 2020, 117, 21014-21021.	7.1	52
21	¹ H-Detected Biomolecular NMR under Fast Magic-Angle Spinning. Chemical Reviews, 2022, 122, 9943-10018.	47.7	51
22	Structure Selectivity of Alkaline Periodate Oxidation on Lignocellulose for Facile Isolation of Cellulose Nanocrystals. Angewandte Chemie - International Edition, 2020, 59, 3218-3225.	13.8	50
23	Proton Association Constants of His 37 in the Influenza-A M2 _{18–60} Dimer-of-Dimers. Biochemistry, 2014, 53, 5987-5994.	2.5	48
24	Proton-Based Structural Analysis of a Heptahelical Transmembrane Protein in Lipid Bilayers. Journal of the American Chemical Society, 2017, 139, 13006-13012.	13.7	47
25	Crucial role for oxygen functional groups in the oxygen reduction reaction electrocatalytic activity of nitrogen-doped carbons. Electrochimica Acta, 2018, 292, 942-950.	5.2	46
26	Structure of AP205 Coat Protein Reveals Circular Permutation in ssRNA Bacteriophages. Journal of Molecular Biology, 2016, 428, 4267-4279.	4.2	45
27	Co-factor-free aggregation of tau into seeding-competent RNA-sequestering amyloid fibrils. Nature Communications, 2021, 12, 4231.	12.8	45
28	ls protein deuteration beneficial for proton detected solid-state NMR at and above 100ÂkHz magic-angle spinning?. Solid State Nuclear Magnetic Resonance, 2017, 87, 126-136.	2.3	45
29	Protein residue linking in a single spectrum for magic-angle spinning NMR assignment. Journal of Biomolecular NMR, 2015, 62, 253-261.	2.8	44
30	Proton Detected Solid-State NMR of Membrane Proteins at 28 Tesla (1.2 GHz) and 100 kHz Magic-Angle Spinning. Biomolecules, 2021, 11, 752.	4.0	43
31	Insights into the molecular mechanism of amyloid filament formation: Segmental folding of α-synuclein on lipid membranes. Science Advances, 2021, 7, .	10.3	43
32	Local and Global Dynamics in <i>Klebsiella pneumoniae</i> Outer Membrane Protein a in Lipid Bilayers Probed at Atomic Resolution. Journal of the American Chemical Society, 2017, 139, 1590-1597.	13.7	41
33	Automated Backbone NMR Resonance Assignment of Large Proteins Using Redundant Linking from a Single Simultaneous Acquisition. Journal of the American Chemical Society, 2020, 142, 5793-5799.	13.7	41
34	Secondary Structure in the Core of Amyloid Fibrils Formed from Human β ₂ m and its Truncated Variant ΔN6. Journal of the American Chemical Society, 2014, 136, 6313-6325.	13.7	40
35	Lipid bilayer-bound conformation of an integral membrane beta barrel protein by multidimensional MAS NMR. Journal of Biomolecular NMR, 2015, 61, 299-310.	2.8	38
36	Magic Angle Spinning Nuclear Magnetic Resonance Characterization of Voltage-Dependent Anion Channel Gating in Two-Dimensional Lipid Crystalline Bilayers. Biochemistry, 2015, 54, 994-1005.	2.5	34

#	Article	IF	CITATIONS
37	Structural and molecular basis of cross-seeding barriers in amyloids. Proceedings of the National Academy of Sciences of the United States of America, 2021, 118, .	7.1	34
38	Efficient resonance assignment of proteins in MAS NMR by simultaneous intra- and inter-residue 3D correlation spectroscopy. Journal of Biomolecular NMR, 2013, 55, 257-265.	2.8	32
39	Imidazole–Imidazole Hydrogen Bonding in the pH-Sensing Histidine Side Chains of Influenza A M2. Journal of the American Chemical Society, 2020, 142, 2704-2708.	13.7	32
40	Structure and reactivity of [(L·Pd) n ·(1,5-cyclooctadiene)] (n = 1–2) complexes bearing biaryl phosphine ligands. Inorganica Chimica Acta, 2014, 422, 188-192.	2.4	30
41	Dynamic Nuclear Polarization of ¹³ C Nuclei in the Liquid State over a 10â€Tesla Field Range. Angewandte Chemie - International Edition, 2019, 58, 1402-1406.	13.8	30
42	Amantadine inhibits known and novel ion channels encoded by SARS-CoV-2 in vitro. Communications Biology, 2021, 4, 1347.	4.4	29
43	Structure, gating and interactions of the voltage-dependent anion channel. European Biophysics Journal, 2021, 50, 159-172.	2.2	28
44	Degree of Biomimicry of Artificial Spider Silk Spinning Assessed by NMR Spectroscopy. Angewandte Chemie - International Edition, 2017, 56, 12571-12575.	13.8	25
45	Probing Membrane Protein Insertion into Lipid Bilayers by Solid‣tate NMR. ChemPhysChem, 2019, 20, 302-310.	2.1	24
46	Determination of Global Structure from Distance and Orientation Constraints in Biological Solids Using Solid-State NMR Spectroscopy. Journal of the American Chemical Society, 2007, 129, 15233-15239.	13.7	23
47	Correcting for magnetic field drift in magic-angle spinning NMR datasets. Journal of Magnetic Resonance, 2019, 305, 1-4.	2.1	22
48	The Molecular Basis of the Interaction of Cyclophilinâ€A with α‧ynuclein. Angewandte Chemie - International Edition, 2020, 59, 5643-5646.	13.8	20
49	Atomic resolution dynamics of cohesive interactions in phase-separated Nup98 FG domains. Nature Communications, 2022, 13, 1494.	12.8	20
50	Alpha protons as NMR probes in deuterated proteins. Journal of Biomolecular NMR, 2019, 73, 81-91.	2.8	19
51	Zuordnung der Rückgrat―und Seitenkettenâ€Protonen in vollstädig protonierten Proteinen durch Festkörperâ€NMRâ€Spektroskopie: Mikrokristalle, Sedimente und Amyloidfibrillen. Angewandte Chemie, 2016, 128, 15730-15735.	2.0	18
52	Catalysis of proline isomerization and molecular chaperone activity in a tug-of-war. Nature Communications, 2020, 11, 6046.	12.8	18
53	Recyclable Ruthenium Catalyst for Distal <i>meta</i> â^'H Activation. Chemistry - A European Journal, 2020, 26, 15290-15297.	3.3	18
54	Helical Fibers via Evaporationâ€Driven Selfâ€Assembly of Surfaceâ€Acylated Cellulose Nanowhiskers. Angewandte Chemie - International Edition, 2018, 57, 16323-16328.	13.8	17

#	Article	IF	CITATIONS
55	Solid-state NMR investigation of the involvement of the P2 region in tau amyloid fibrils. Scientific Reports, 2020, 10, 21210.	3.3	16
56	Structure and Gating Behavior of the Human Integral Membrane Protein VDAC1 in a Lipid Bilayer. Journal of the American Chemical Society, 2022, 144, 2953-2967.	13.7	14
57	Spontaneous Enhancement of Magnetic Resonance Signals Using a RASER. Angewandte Chemie - International Edition, 2021, 60, 20984-20990.	13.8	13
58	Towards a native environment: structure and function of membrane proteins in lipid bilayers by NMR. Chemical Science, 2021, 12, 14332-14342.	7.4	12
59	Poreâ€Bound Water at the Key Residue Histidineâ€37 in Influenzaâ€Aâ€M2. Angewandte Chemie - Internat Edition, 2021, 60, 24075-24079.	ional 13.8	12
60	High-resolution solid-state NMR structure of Alanyl-Prolyl-Glycine. Journal of Magnetic Resonance, 2009, 200, 95-100.	2.1	11
61	Macroscalar Helices Coâ€Assembled from Chiralityâ€Transferring Temperatureâ€Responsive Carbohydrateâ€Based Bolaamphiphiles and 1,4â€Benzenediboronic Acid. Angewandte Chemie - International Edition, 2021, 60, 9712-9718.	13.8	10
62	Resonance assignment of the outer membrane protein AlkL in lipid bilayers by proton-detected solid-state NMR. Biomolecular NMR Assignments, 2020, 14, 295-300.	0.8	9
63	Transferred-Rotational-Echo Double Resonance. Journal of Physical Chemistry A, 2021, 125, 754-769.	2.5	9
64	Modest Offset Difference Internuclear Selective Transfer via Homonuclear Dipolar Coupling. Journal of Physical Chemistry Letters, 2022, , 1540-1546.	4.6	9
65	Direct nitrogen interception from chitin/chitosan for imidazo[1,5- <i>a</i>]pyridines. Chemical Communications, 2022, 58, 6068-6071.	4.1	8
66	Direct Detection of Bound Ammonium Ions in the Selectivity Filter of Ion Channels by Solid-State NMR. Journal of the American Chemical Society, 2022, 144, 4147-4157.	13.7	7
67	Spontaneous Enhancement of Magnetic Resonance Signals Using a RASER. Angewandte Chemie, 2021, 133, 21152-21158.	2.0	5
68	Degree of Biomimicry of Artificial Spider Silk Spinning Assessed by NMR Spectroscopy. Angewandte Chemie, 2017, 129, 12745-12749.	2.0	4
69	Centerbandâ€Only Detection of Exchange NMR with Naturalâ€Abundance Correction Reveals an Expanded Unit Cell in Phenylalanine Crystals. ChemPhysChem, 2020, 21, 1622-1626.	2.1	4
70	Dynamic Nuclear Polarization of ¹³ C Nuclei in the Liquid State over a 10â€Tesla Field Range. Angewandte Chemie, 2019, 131, 1416-1420.	2.0	3
71	Heteronuclear and homonuclear radio-frequency-driven recoupling. Magnetic Resonance, 2021, 2, 343-353.	1.9	3
72	Membrane-embedded TSPO: an NMR view. European Biophysics Journal, 2021, 50, 173-180.	2.2	3

#	Article	IF	CITATIONS
73	Frontispiece: NMR Spectroscopic Assignment of Backbone and Side-Chain Protons in Fully Protonated Proteins: Microcrystals, Sedimented Assemblies, and Amyloid Fibrils. Angewandte Chemie - International Edition, 2016, 55, .	13.8	2
74	The Small Molecule anle138b Shows Interaction with α-Synuclein Oligomers in Phospholipid Membranes. Biophysical Journal, 2018, 114, 560a.	0.5	2
75	Protein-Drug Interactions in the Membrane: The Small Molecule Anle138b and its Binding to α-Synuclein Oligomers. Biophysical Journal, 2019, 116, 352a.	0.5	2
76	Backbone Torsion Angle Determination Using Proton Detected Magic-Angle Spinning Nuclear Magnetic Resonance. Journal of Physical Chemistry Letters, 2022, 13, 18-24.	4.6	2
77	Orphan spin operator diagonal suppression. Journal of Magnetic Resonance Open, 2022, 10-11, 100025.	1.1	1
78	Investigating VDAC Gating via Magic Angle Spinning NMR and Electrophysiological Measurements Under Extreme pH Conditions: Implications for the Voltage-Gating Mechanism. Biophysical Journal, 2011, 100, 8a-9a.	0.5	0
79	The Molecular Basis of the Interaction of Cyclophilinâ€A with αâ€ S ynuclein. Angewandte Chemie, 2020, 132, 5692-5695.	2.0	0
80	Centerbandâ€Only Detection of Exchange NMR with Naturalâ€Abundance Correction Reveals an Expanded Unit Cell in Phenylalanine Crystals. ChemPhysChem, 2020, 21, 1621-1621.	2.1	0
81	Pore bound water at the key residue histidineÂ37 in Influenza A M2. Angewandte Chemie, 2021, 133, 24277.	2.0	0